A density functional theory study of adsorption and dissociation of H2 molecule on small PdnAgm (n + m ≤ 4) metal clusters

Faisal Al-Odail (falodail@kfu.edu.sa)
King Faisal University https://orcid.org/0000-0002-5434-3397
Javed Mazher
King Faisal University

Research Article

Keywords: Bimetallic clusters, Pd-Ag small clusters, DFT, Hydrogen adsorption and dissociation

Posted Date: April 26th, 2022

DOI: https://doi.org/10.21203/rs.3.rs-1516797/v1

Abstract

The adsorption and dissociation of hydrogen molecule on small Pd_nAg_m ($n + m \leq 4$) clusters is studied employing density functional theory (DFT) calculations. The lowest energy structures of the Pd_nAg_m clusters are initially presented. Based on the obtained structures, various geometries of H_2 adorption and dissociation with these clusters are examined. The cluster size and composition of the Pd_nAg_m clusters are found to control the nature of the adsorption process. The results suggest that molecular adsorption is more favourable on the Pd atom and mixed clusters, while hydrogen dissociation is more favourable on the Pd_n ($n = 2–4$) clusters. The Pd dimer and trimer are found to be the most reactive clusters for hydrogen adsorption, while single Ag atom is the least reactive one. The natural bond orbital (NBO) population analysis indicates that hydrogen atoms tend to draw electrons from the metal clusters in the dissociative form and donate electrons to the metal clusters in the molecular adsorption form. The density of states (DOS) of the Pd_nAg_m trimers are also presented and discussed.

1. Introduction

A metal cluster can be defined as aggregates of a small number to hundreds of atoms. This class of materials possesses high surface to volume ratio compared to their bulk counterparts reflecting distinctive physical and chemical properties [1, 2]. The geometric structure and size of small transition metal clusters play a key role in controlling their behaviour [3]. Consequently, the catalytic properties of small metallic clusters are expected to vary and be sensitive to the cluster size and composition [4]. Adding an impurity atom or alloying can further modify the physical and chemical properties of pure transition metal clusters affecting their catalytic properties [4–6]. Typically, the presence of the second component is expected to change the electronic and geometric properties and enhances the catalytic performance of monometallic catalysts [5–7]. The enhanced activity of bimetallic catalysts could be attributed to "geometric ensemble effects" where by active sites on the catalyst surface consist of atoms arranged in specific groupings [7].

The study of interactions between transition metal clusters with atoms or small molecules is fundamental to understand catalytic processes. A primary step to the reaction mechanism is the adsorption behavior of the atoms or small molecules on the metal clusters [6, 8, 9]. Hydrogen possesses the characteristics of being abundant, high energy content material, eco-friendly and renewable that makes it a candidate alternative to fossil fuels and a potential energy source [10, 11]. The interactions and behavior of hydrogen on metal surfaces and clusters are of importance to various applications and technologies such as catalytic processes, metal embrittlement, hydrogen storage and fuel cells [11–15]. In the latter case, for instance, electricity can be generated by harmless electrochemical reactions of hydrogen and oxygen on metal surfaces as catalysts; and the process typically involves the adsorption and diffusion of the constituents. For example, proton conducting fuel cells employ an acidic media and hydrogen gas as a fuel, and consequently hydrogen oxidation occurs at the anode producing electrons and protons which migrate to the cathode and recombine with oxygen resulting in water [11, 14, 16].

The electronic structure of hydrogen atoms and molecules is simple. Therefore, electronic structure methods can be effectively employed to describe their interactions with metal surfaces and provide valuable insights into essential properties of hydrogen-metal systems such as surface reactivity, bond-making and bond-breaking

behaviors [17]. In this regard, a number of theoretical studies have been carried out on the interactions between atomic or molecular hydrogen with pure and/or binary metal clusters [5, 6, 8, 9, 13, 14, 18–29]. It has been largely proposed that the nature of the metallic components, geometry and size are crucial in controlling the adsorption and dissociation behaviors of hydrogen on the binary cluster surfaces.

A series of Pd-Ag bimetallic catalysts have experimentally been shown to be efficient for methane combustion [30], oxidation of carbon monoxide [31], partial hydrogenation of acetylene [32], dehydrogenation of formic acid [33, 34] and fuel cell-related reactions [35–37]. Pd-Ag binary alloys have also been acknowledged as efficient and promising materials for hydrogen gas permeation and storing [38–41] as well as sensing [42]. Additionally, various physiochemical properties of Pd-Ag bimetallic cluster system have been estimated by theoretical calculations [3, 43–45]. For instance, a DFT study of small Pd_nAg (n = 1–8) clusters [45] has indicated that the $Pd_{3-8}Ag$ clusters possess three-dimensional configurations and their binding energies are nearly similar to that of the corresponding Pd_n clusters. The study has also found that stability and reactivity of the ground-state clusters are size-dependent, and that a universal charge transfer takes place from Ag atom to Pd atoms within the clusters. It has also been shown for Ag_m-Pd_n (m + n = 5) clusters that structures of bimetallic tetramers and pentamers shift from two to three dimensions with the presence of two Pd atoms in the cluster. Besides, stability analysis of the bimetallic tetramers has revealed that Ag_2Pd_2 is the most stable cluster [3]. Other theoretical studies have focused on the assessment of various chemical processes over Pd-based [46–48], Pd-doped and Ag-doped surfaces [49, 50]. Furthermore, a recent DFT study by Yang et.al. has examined the HCOOH decomposition over pure and Ag-modified Pd nanoclusters [51]. The study suggests that the activity and selectivity of the process can be improved by controlling the size and Ag composition of the nanoclusters.

A particular attention has also been directed towards studying the interactions of small molecules with Pd-Ag binary clusters. Zhao et.al. have indicated that a preferential binding of both CO [52] and NO [53] molecules takes place on Pd sites when both elements co-exist in the cluster. The authors have also found that the binding energy in both cases increases with increasing Pd content in the cluster. A study of Ag_nPdH ($n \leq 5$) clusters [21] has shown that hydrogen atom binds to Ag-Pd bridge site when (n = 1–4) and to top site in the case of Ag_5Pd.

It has also been verified that hydrogen molecule adsorbs more favorably and dissociates more easily at Pd atom than Ag atom on the PdAg dimer [19, 23]. The dissociation behavior of hydrogen molecule on Ag_5 and Pd_5 clusters has been compared by Bartczak and Stawowska to that on Ag_4Pd and $AgPd_5$ clusters [8]. The authors have suggested that the molecule dissociates on Pd_5 cluster, while no dissociation occurs on Ag_5 cluster. The study has also concluded that mixing Ag with pure Pd catalyst reduces its ability for hydrogen dissociation, while mixing Pd with pure Ag enhances its ability for the dissociation process. Moreover, Zhang and Yang [29] have shown that, among $Pd_nAg_{(8-n)}$ alloy clusters, Pd_5Ag_3 and Pd_2Ag_6 provide promising candidates for hydrogen dissociation and storage processes respectively. A variety of other DFT studies have focused on the evaluation of the catalytic performance of Pd-Ag clusters for hydrogenation of acetylene [54, 55] and CO oxidation [56]. These studies broadly suggest that mixing the two elements enhances the adsorption properties of the reactant molecules on the bimetallic clusters leading to a better performance in comparison with the mono-component clusters.

This work aims to systematically address the adsorption and dissociation behavior of hydrogen molecule on Pd_nAg_m ($n + m \leq 4$) clusters within the frame work of density functional theory (DFT) at the B3P86/Lanl2DZ

level of theory. Initially, the lowest energy structures of Pd_nAg_m clusters are presented. Then, a number of structural and electronic properties of most stable structures of Pd_nAg_m-H_2 clusters are presented and discussed.

2. Computational Method

All the calculations presented in this work are carried out using Gaussian 09 software [57]. GauusView 05 [58] is used for drawing atomic and molecular structures of Pd_nAg_m and Pd_nAg_m-H_2 clusters and results visualization. B3P86 exchange correlation functional and Lanl2DZ basis set are used for Pd and Ag atoms, while the 6-311 + + G(d,p) basis set is used for hydrogen atoms. The B3P86/Lanl2DZ level of theory has recently been shown to be reliable for the assessment of small Pd_nAg (n = 1–8) clusters [45]. The reliability of this method for the study of molecular hydrogen adsorption on Pd_nAg_m clusters has been initially assessed by calculating the binding energies, bond lengths and vibrational frequencies of Pd_2, Ag_2, PdAg, PdH, AgH and H_2 dimers at the B3P86 / Lanl2DZ level of theory alongside the PW91PW91 and B3LYP methods. The PW91PW91 method has been previously employed for the study of CO and NO bindings on small Ag_nPd_m clusters [52, 53] and atomic hydrogen interaction with Ag_nPd clusters [21]. In addition, the B3LYP method has been used for the study of molecular hydrogen interaction with various transition metal homonuclear and heteronuclear dimers [19]. The calculated parameters of the dimers are shown in Table 1 alongside other theoretical data from the literature and the corresponding experimental values; the blank values are not available to the best of the authors' knowledge. In comparison with the other two functionals, the results obtained with B3P86 method are largely closer to the experimental values. Besides, the calculated parameters using the B3P86 functional are consistent with the theoretical findings from other published works [3, 18, 19, 22–24, 59–61]. Hence, the results in the table suggest that the B3P86 is an effective method for the evaluation of hydrogen adsorption on Pd_nAg_m clusters.

The study of the H_2 adsorption and dissociation on Pd_nAg_m ($n + m \leq 4$) clusters is accomplished by, first, optimizing various possible geometries of the clusters to identify the lowest energy structures. Then, a variety of possible configurations of the adsorption and dissociation of hydrogen molecule on the most stable configurations of Pd_nAg_m clusters are optimized to identify the lowest energy structures. The most stable geometries of the Pd_nAg_m and Pd_nAg_m-H_2 clusters are determined by performing structural optimization and vibrational frequency calculations for each structure at different spin multiplicities. Natural bond orbital (NBO) analysis is carried out for the Pd_nAg_m-H_2 clusters at the B3P86/Lanl2DZ level of theory to investigate the charge distributions. The DOS analysis is carried out using the GaussSum software [62].

3. Results And Discussions

3.1. Geometrical structures of Pd_nAg_m clusters

Initially, the lowest energy structures up to four atoms of pure Pd, Ag and bimetallic Pd_nAg_m clusters are determined by optimizing various possible structures at B3P86/Lanl2DZ level of theory and different spin multiplicities. ***Figure 1*** shows the obtained results arranged in the order of decreasing Pd content in the cluster. The lowest energy structures of pure Pd clusters are obtained with triplet spin state apart from the single atom. On the other hand, the ground states of pure Ag and bimetallic Pd_nAg_m clusters are found to be in the singlet

and doublet spin multiplicities respectively. It is clear from the figure that the lowest energy structure of pure and bimetallic trimers is an isosceles triangle, while that of pure Pd and Ag tetramers are distorted tetrahedron and rhombus respectively. The calculations also show that the ground state configurations of both Pd_3Ag and Pd_2Ag_2 clusters are similar to that of Pd_4, while that of $PdAg_3$ cluster is similar to that of Ag_4 indicating that the elemental content dominates the configuration of the Pd_nAg_m tetramer. Similar structural properties have been previously reported for Ag-Pd clusters [3, 52].

Based on the obtained ground state structures of pure and bimetallic clusters, numerous geometries of molecular hydrogen adsorption and dissociation on these clusters were examined at the same level of theory and two spin multiplicities (singlet and triplet or doublet and quartet) in order to predict the lowest energy structures. ***Figure 2*** reveals the optimized ground state geometries (denoted as a) alongside other low-lying isomers (denoted as b-f) of Pd_nAg_m-H_2 clusters arranged from the highest to lowest Pd content in the cluster and lowest to highest energy structures. Also, the spin multiplicity, adsorption energy, average bond length, M-M bond length, shortest M-H bond length, H-H bond length, sum of NBO net charges of hydrogen atoms and HOMO-LUMO energy gap of the lowest energy structures are presented in ***Tables 2-5***. It can be noted from these tables that the ground state geometries in all cases are obtained with the lowest spin multiplicity, that is singlet or doublet.

3.2. Molecular hydrogen interaction with Pd_nAg_m clusters

On the Pd atom, molecular hydrogen adsorption takes place without dissociation forming the ground state of Pd-H_2 cluster (PdH_2_a). The shortest Pd-H, H-H distances, H-Pd-H angle and H-H vibrational frequency in this cluster are 1.661 Å, 0.881 Å, 30.76° and 2764.39 cm^{-1} respectively. Isomer PdH_2-b, in which molecular hydrogen dissociation occurs, is less stable and higher in energy than the ground state by 0.197 eV. This suggest that an energy barrier of the latter value is required for the transformation from the molecular to dissociative adsorption of hydrogen on the Pd atom. Isomer PdH_2_c is much less stable than the lowest energy structure and found to be higher in energy by 2.415 eV. The obtained results for PdH_2_a and PdH_2_b are comparable to previous theoretical findings [22]. On the other extreme, the ground state geometry on the Ag atom (AgH_2_a) involves molecular hydrogen dissociation with Ag-H, H-H distances and H-Ag-H angle of 1.660 Å, 2.840 Å and 117.59° respectively. The linear structure (AgH_2_b) is less stable and found to be higher in energy than AgH_2_a by 0.390 eV. The atomic configuration of Pd is a closed-shell of $4d^{10}$, while that of Ag is $4d^{10}$ $5s^1$ which means that it has only one *s* valence electron [22, 24]. This could be the reason of the better reactivity on Ag atom towards hydrogen dissociation.

The interaction behaviour on homonuclear dimers is contrary to that on single atoms. Apparently, H_2 prefers to dissociate into two hydrogen atoms at the bridge sites of Pd_2 forming the lowest energy structure (Pd_2H_2_a) with Pd-Pd and shortest Pd-H bond lengths of 2.699 Å and 1.661 Å. This geometry has also been proposed by Ni and Zeng [22] as the ground state of Pd_2H_2 cluster with comparable bond lengths to that obtained in this work. Pd_2H_2_b geometry is higher in energy than the ground state by 0.818 eV. In this geometry, hydrogen molecule binds to the bridge site of the Pd_2 dimer with H-H bond distance of 1.036 Å which is longer than the corresponding experimental value 0.746 Å [19] suggesting more tendency of H_2 towards dissociation. Isomer Pd_2H_2_c is less stable structure than the previous two structures and found to have a higher energy than the

ground state by 1.501 eV. This structure involves molecular hydrogen adsorption on top of one Pd atom in line with the axis of Pd_2 dimer with Pd-H and H-H bond lengths of 1.681 Å and 0.870 Å which are close to findings in other reports [14, 22, 27]. Similarly, H_2 prefers to molecularly adsorb on top of one Ag atom in line with the axis of Ag_2 dimer forming the ground state structure (Ag_2H_2_a) with Ag-Ag, Ag-H and H-H bond lengths of 2.573 Å, 2.519 Å and 0.751 Å respectively. These results suggest that H_2 tends to weakly bind to Ag_2 dimer and are in harmony with previous observations by Wang et.al [19]. The dissociative form (Ag_2H_2_b), in which one hydrogen atom is placed at the bridge sites, is less stable geometry and found to be higher in energy than the ground state by 1.425 eV.

On the heteronuclear cluster, molecular adsorption appears to be more favourable than the dissociative adsorption with lower energy when the molecule binds to Pd site. The lowest energy structure is obtained with H_2 molecule horizontally placed on the top of Pd atom ($PdAgH_2$_a) with H-Pd-H angle of 28.77°. When H_2 molecule is placed on top of Pd atom in line with the axis of the PdAg dimer, another stable structure ($PdAgH_2$_b) is obtained which is higher in energy than the ground state by 0.117 eV. In contrast, placing H_2 molecule on top of Ag atom forms a lesser stable structure ($PdAgH_2$_c) with energy higher than the ground state by 0.467 eV. The Ag-H bond length in the latter case is much longer than the Pd-H bond length in the former case which also indicates, as in the case of the Ag_2 dimer, that H_2 molecule tends to physically adsorb on the PdAg dimer when attached to the Ag site in the bimetallic cluster. A similar behaviour of hydrogen adsorption on Ag_2 and PdAg clusters has been stated previously [19]. In the dissociative form, hydrogen atoms prefer binding to the bridge sites of the PdAg cluster ($PdAgH_2$_d) rather than one atom at the bridge site and the other at the Pd or Ag site ($PdAgH_2$_e and $PdAgH_2$_f). These structures are found to be higher in energy than the lowest energy structure by 0.389, 0.398 and 0.609 eV respectively.

For H_2 interaction with Pd_3 trimer, the dissociation process is more favoured than the molecular adsorption. The ground state structure is obtained with one hydrogen atom located at the bridge site and the other one at the face of the isosceles triangle (Pd_3H_2_a). The total energy of the next geometrical structures with one hydrogen atom at each face of the triangle (Pd_3H_2_b) and two hydrogen atoms at the bridge sites (Pd_3H_2_c) are found to be in close proximity to that of the ground state with a difference of only 0.008 and 0.07 eV respectively. Similar results have been proposed by Ni and Zeng [22]. However, the authors suggest that the structure that involves two hydrogen atoms at the bridge sites is the ground state structure of this system. Isomer Pd_3H_2_d involves molecular hydrogen adsorption on the top of one Pd atom with much higher energy than the ground state by 1.404 eV. The lowest energy structure on Ag_3 cluster is obtained by molecular adsorption on the top of a silver atom with Ag-H and H-H bond lengths of 2.218 and 0.761 Å (Ag_3H_2_a). The molecular dissociation into two hydrogen atoms at the bridge sites (Ag_3H_2_b) is less favoured structure and found to be higher in energy than the ground state by 0.226 eV.

The elemental content of the bimetallic trimer controls its behaviour towards hydrogen adsorption. The calculations suggest that H_2 molecule prefers to dissociate on Pd_2Ag trimer, while the molecular adsorption is more favoured on $PdAg_2$ trimer. Apparently, the adsorption behaviour on the Pd_2Ag and $PdAg_2$ is similar to that on pure Pd_3 and Ag_3 trimers suggesting that doping pure clusters with only one atom from the other constituent does not change their tendency towards adsorbing hydrogen molecule. The lowest energy structure on the Pd_2Ag trimer (Pd_2AgH_2_a) is obtained by placing the two hydrogen atoms at the bridge sites of Pd-Pd. The next

isomers (Pd_2AgH_2_b, Pd_2AgH_2_c, Pd_2AgH_2_d and Pd_2AgH_2_e) are found to be in order higher in energy than the ground state by 0.140, 0.163, 0.175 and 0.455 eV. On the $PdAg_2$ trimer, the ground state is obtained by molecular adsorption at Pd site with Pd-H, H-H bond lengths and H-Pd-H angle of 1.730 Å, 0.840 Å and 28.09° respectively. Calculations have also shown that ($PdAg_2H_2$_b, $PdAg_2H_2$_c, $PdAg_2H_2$_d, $PdAg_2H_2$_e and $PdAg_2H_2$_f) configurations are less stable than the ground state.

In a similar manner to the behaviour on dimers and trimers, hydrogen molecule favours dissociation on the Pd tetramers. The ground state configuration (Pd_4H_2_a) is obtained by placing one hydrogen atom at two triangle faces of the Pd_4 tetrahedron structure. This structure is more stable than that with two hydrogen atoms placed at the bridge sites (Pd_4H_2_b) with energy difference of 0.035 eV. Molecular hydrogen adsorption (Pd_4H_2_c) is also obtained with 0.820 eV energy difference apart from the ground state. The calculations also suggest, only for this configuration, that the triplet spin multiplicity is lower in energy than the singlet spin state by 0.664 eV. On the Ag tetramers, molecular hydrogen dissociation is more preferred with one hydrogen atom at the two-fold bridge sites of the rhombus structure (Ag_4H_2_a) and shortest Ag-H bond length of 1.816 Å. This is in line with previous observations of atomic hydrogen interaction with Ag_4 cluster [9, 24]. The next isomer (Ag_4H_2_b) involves molecular hydrogen adsorption with total energy higher than that of the ground state by 0.291 eV. Structure (Ag_4H_2_c) is obtained with the triplet spin state and its energy is higher than (Ag_4H_2_a) by 1.626 eV.

The adsorption behaviour of hydrogen molecule on the bimetallic Pd_nAg_m tetramers is different from that on the corresponding mono-component tetramers. For Pd_3Ag and Pd_2Ag_2 clusters, the ground states are obtained with molecular adsorption at Pd site in the distorted tetrahedron structure (Pd_3AgH_2_a and $Pd_2Ag_2H_2$_a). On the $PdAg_3$ cluster, the ground state is also obtained by molecular adsorption at Pd site in the rhombus structure. This is unlike the behaviour on the corresponding Pd_4 and Ag_4 clusters where molecular dissociation is more preferred (Pd_4H_2_a and Ag_4H_2_a) indicating that doping Pd tetramers with one or two Ag atoms, and doping Ag tetramers with one Pd atom interfere their affinity towards dissociating hydrogen molecule.

Figure 3 illustrates the shortest M-H bond lengths of the ground state geometries of Pd_nAg_m-H_2 clusters. Apparently, the bond lengths in the case of Ag single atom, pure Pd and bimetallic Pd_nAg_m clusters are in close proximity and found to be in the range between 1.650-1.758 Å. The Ag-H bond length is longer in pure Ag clusters with significant peaks appearing at Ag_2H_2 and Ag_3H_2 clusters. It is also noticeable from the results in the ***Tables 2-5*** that Pd-H bond length is mostly shorter than that of Ag-H which suggests a stronger interaction in the case of Pd-H.

The average Pd-Ag bond lengths (R_{ABL}) of the lowest energy structures of Pd_nAg_m clusters before and after hydrogen adsorption are also shown in ***Figure 4***. It is obvious from the figure that the dissociative adsorption increases the R_{ABL} of the entire cluster, while, with exception in the case of Pd-Ag cluster, no significant change occurs upon the molecular adsorption indicating that the former type of adsorption weakens the atomic interactions in the cluster. These results are consistent with the suggestion by Zhao et.al that dissociative adsorption of hydrogen greatly changes the geometry of Au_nPd_m cluster [27].

3.3. Adsorption Energies

The adsorption energy (E_{ads}) of the Pd_nAg_m-H_2 cluster system is calculated using the formula [13, 24, 27]:

$$E_{ads} = E_{PdnAgm} + E_{H2} - E_{PdnAgm\text{-}H2}$$

where E_{PdnAgm}, E_{H2}, $E_{PdnAgm\text{-}H2}$ are the total energies of the Pd_nAg_m, H_2 and hydrogen molecule adsorbed on Pd_nAg_m clusters respectively. A more positive value of E_{ads} is a sign for a stronger bond [27]. The E_{ads} for the ground state geometries of Pd_nAg_m-H_2 clusters are displayed in ***Figure 5***. The results reveal that the E_{ads} of pure Pd clusters are higher than the corresponding Ag clusters which is also another evidence for a stronger interaction of hydrogen with Pd atoms as compared to Ag atoms. For the bimetallic clusters, the adsorption energies are between that of pure clusters suggesting that doping Ag clusters with Pd atoms enhances their interaction with hydrogen and inversely doping Pd clusters with Ag atoms weakens their interaction with hydrogen. The data in the figure also suggest that Pd dimer and trimer are the most reactive clusters for hydrogen adsorption, while single Ag atom is the least reactive one. Besides, the values in ***Tables 2-5*** show that the E_{ads} for a given bimetallic cluster and geometry is much greater when the hydrogen atoms are around Pd site. Similar trends have been previously reported for CO and NO interactions with Ag_nPd_m clusters [52, 53]. Based on the adsorption energies presented for the ground states in ***Tables 2-5***, it appears that molecular adsorption is more favourable on the Pd atom and mixed clusters, while the Pd_n (2-4) clusters are more appropriate for hydrogen dissociation.

3.4. Charge Transfer

It has recently been shown for small Pd_nAg clusters that a charge transfer from Ag atom to Pd atoms takes place indicating that Ag atom acts as electron donor and Pd atom acts as an electron acceptor within the clusters [45]. This behaviour can be linked to the fact that Pd is more electronegative than Ag (2.20 and 1.93) resulting in larger electron population and a stronger interaction with the adsorbed molecule at Pd site [52, 53].

The NBO population analysis suggests that the charge distribution within the lowest energy structures of Pd_nAg_m-H_2 clusters depends on the nature of hydrogen adsorption. With exception in the case of single Pd atom, one can observe from the data presented in ***Tables 2-5*** that hydrogen atoms possess negative charge in the dissociative adsorption and positive charge in the molecular adsorption. This indicates that hydrogen atoms tend to draw electrons from the metal clusters in the dissociative form, while they tend to donate electrons to the metal clusters in the molecular adsorption form. The charge transfer tendency within the Pd_nAg_m-H_2 clusters is similar to the case of H_2 interaction with Au_nPd_m clusters [27]. Ni and Zeng [22] have also indicated for H_2 adsorption on Pd_n clusters that a charge transfer from Pd atoms to hydrogen takes place in the dissociative form.

3.5. HOMO-LUMO energy gap

The chemical stability and reactivity of nanoclusters can be evaluated by the HOMO-LUMO energy gap (E_{gap}). A larger value of the E_{gap} indicates higher chemical stability and lower chemical reactivity [59, 60]. The E_{gap} of the ground state structures of Pd_nAg_m-H_2 clusters alongside the corresponding values of the Pd_nAg_m clusters are represented in ***Figure 6***. The energy gaps of the adsorbed single atoms and dimers are higher than that of the Pd_nAg_m clusters. For the trimers and tetramers, the gaps decrease monotonically with increasing the Ag content in the cluster before hydrogen adsorption and oscillate after the adsorption process. A maximum E_{gap} occurs in

the case of Ag-H_2 cluster, while the Ag_3-H_2 cluster exhibits the smallest E_{gap} indicating that it tends to be relatively less stable and more reactive among the examined systems. Besides, the Ag atom has the lowest chemical reactivity which is in harmony with the result in ***Figure 5*** that Ag atom is the least reactive for hydrogen adsorption.

The E_{gap} of the Pd_nH_2 cluster decreases with increasing the Pd content in the cluster, while no similar tendency can be observed for Pd_n or Ag_m and Ag_m-H_2 clusters. Ni and Zeng [22] have also reported similar findings for Pd_nH_2 and Pd_n clusters.

3.6. DOS Analysis

To further analyse the electronic properties of hydrogen interaction with Pd_nAg_m clusters, the electronic density of state (DOS) spectra of the trimers as a representative system of the others is shown in ***Figure 7*** as well as the DOS spectrum of hydrogen molecule in the gas phase. A number of remarkable DOS peaks can be observed in the vicinity of the Fermi level in the energy range 5 to -5 eV. It is clear from the figure that the Fermi level for pure Pd_3 and heteronuclear Pd_2Ag clusters is less populated. The interaction with H_2 increases the density of state near Fermi level of these clusters and that changes their electronic structures due to charge transfer from hydrogen atoms to the cluster. Moreover, the net charges of hydrogen atoms as shown in Table 4 for these clusters are - 0.266 e and - 0.300 e, respectively, implying more electrons are gained by the cluster. This can be ascribed to the decreased M-H bond lengths as shown in Figure 3 which facilitates more amount of charge transfer to the cluster. Also, the large density of state near the Fermi level after the interaction with hydrogen is manifested in lowering of the Homo-Lumo gap as shown in Figure 6 for these cluster. On the contrary, the charge transfer is very small in pure Ag_3 and $PdAg_2$ clusters as can be seen from Table 4. Therefore, the Homo-Lumo gap and DOS at the Fermi level are not changing significantly in these clusters as a result of the interaction with hydrogen atoms. Thus, it is interesting to note that molecular hydrogen adsorption is taking place in the latter two clusters with the R_{H-H} values 0.761 and 0.837 Å respectively. On the other hand, the dissociative adsorption is taking place in the former two clusters as shown in Table 4. Similar trends of large change in the Homo-lumo gap and electronic structure during the molecular and dissociative adsorption of hydrogen molecule on Au_nPd_m bimetallic clusters has been reported by Zhao et.al. [27]. Furthermore, higher interaction of hydrogen atoms with the metal clusters occurs when the adsorption energies are high [29]. The obtained adsorption energies for the trimers are in the order Pd_3 > Pd_2Ag > $PdAg_2$ > Ag_3 as shown in ***Figure 5***. Therefore, the electronic structure is more affected in the clusters with large adsorption energies as shown by the density of states for Pd_3-H_2 and Pd_2Ag-H_2 clusters in Figure 7.

4. Conclusion

DFT calculations have been carried out in this study to systematically investigate the adsorption and dissociation of hydrogen molecule on small Pd_nAg_m ($n + m \leq 4$) clusters. The ground state geometries of the Pd_nAg_m clusters are initially determined by optimizing various possible structures. Based on the obtained geometries, the lowest energy structures of Pd_nAg_m-H_2 clusters have been identified by optimizing several possible configurations of molecular hydrogen adsorption and dissociation on the most stable configurations of Pd_nAg_m clusters. The results have revealed that the nature of the adsorption process is controlled by the size and composition of the clusters. Molecular adsorption has been found to be more favourable on the Pd atom

and mixed clusters, while hydrogen dissociation is more favourable on the Pd_n (n = 2–4) clusters. The adsorption energy calculations have shown that hydrogen interacts more strongly with Pd atoms than Ag atoms. It has also been found that hydrogen interaction with Ag clusters can be enhanced by doping with Pd atoms, while inversely doping Pd clusters with Ag atoms weakens their interaction with hydrogen. The study has revealed that the Pd dimer and trimer are the most reactive clusters for hydrogen adsorption, while single Ag atom is the least reactive one. The NBO population analysis has shown that electrons transfer from the metal clusters to hydrogen atoms in the dissociative form and from hydrogen atoms to the metal clusters in the molecular adsorption form. The DOS analysis of the trimers has shown that Pd_3 cluster possesses higher d density of state close to the Fermi level compared to the other systems resulting in higher adsorption energy.

Declarations

Acknowledgments

The authors would like to thank the Deanship of Scientific Research at King Faisal University for funding this work under the project (160061).

Funding

This work was supported by the Deanship of Scientific Research at King Faisal University Grant number (160061).

Competing Interests

The authors have no relevant financial or non-financial interests to disclose

Author Contributions

All authors contributed to the study conception and design. Material preparation, data collection and analysis were performed by Faisal Al-Odail, and Javed Mazher. The first draft of the manuscript was written by Faisal Al-Odail, and Javed Mazher and all authors commented on previous versions of the manuscript. All authors read and approved the final manuscript.

Data Availability

The datasets generated during and/or analysed during the current study are available from the corresponding author on reasonable request.

References

1. W. Eberhardt, Surface Science, 500 (2002) 242.
2. N.B. Singh and U. Sarkar, Molecular Simulation, 40 (2014) 1255.
3. D.A. Kilimis and D.G. Papageorgiou, Journal of Molecular Structure: THEOCHEM, 939 (2010) 112.
4. S. Chretien, S. Buratto and H. Metiu, Current Opinion in Solid State and Materials Science, 11 (2007) 62.

5. N.S. Venkataramanan, A. Suvitha, H. Mizuseki and Y. Kawazoe, International Journal of Quantum Chemistry, 113 (2013) 1940.
6. L. Ma, J. Wang, Y. Hao and G. Wang, Computational Materials Science, 68 (2013) 166.
7. F. Maroun, F. Ozanam, O.M. Magnussen and R.J. Behm, Science, 293 (2001) 1811.
8. W.M. Bartczak and J. Stawowska, Structural Chemistry, 15 (2004) 447.
9. X. Lou, H. Gao, W. Wang, C. Xu, H. Zhang and Z. Zhang, Journal of Molecular Structure: THEOCHEM, 959 (2010) 75.
10. J. Wang, J. Liu, B. Zhang, X. Ji, K. Xu, C. Chen, L. Miao and J. Jiang, Phys. Chem. Chem. Phys., 19 (2017) 10125.
11. E.d.V. Gómez, S. Amaya-Roncancio, L.B. Avalle, D.H. Linares and M.C. Gimenez, Applied Surface Science, 420 (2017) 1.
12. P. Ferrin, S. Kandoi, A.U. Nilekar and M. Mavrikakis, Surface Science, 606 (2012) 679.
13. L. Guo and Y. Yang, International Journal of Hydrogen Energy, 38 (2013) 3640.
14. I. Kaul and P. Ghosh, Chemical Physics, 487 (2017) 87.
15. C.C. Boungou, G.B. Bouka-Pivoteau, B.R. Malonda-Boungou, M. N'dollo, P.S. Moussounda, A.T. Raji and E. Kanga, Computational Condenced Matter, 28 (2021) e00582.
16. L. Carrette, K.A. Friedrich and U. Stimming, ChemPhysChem, 1 (2000) 162.
17. A. Groß, Surface Science, 606 (2012) 690.
18. J.O.M.A. Lins and M.A.C. Nascimento, Chemical Physics Letters, 391 (2004) 9.
19. M.Y. Wang, X.J. Liu, J. Meng and Z.J. Wu, Journal of Molecular Structure: THEOCHEM, 804 (2007) 47.
20. Z.J. Li and J.H. Li, Solid State Communications, 149 (2009) 375.
21. S. Zhao, Y. Ren, Y. Ren, J. Wang and W. Yin, International Journal of Quantum Chemistry, 111 (2011) 2428.
22. M. Ni and Z. Zeng, Journal of Molecular Structure: THEOCHEM, 910 (2009) 14.
23. P. Matczak, Reaction Kinetics, Mechanisms and Catalysis, 102 (2011) 1.
24. X. Kuang, X. Wang and G. Liu, Structural Chemistry, 22 (2011) 517.
25. M. Samolia and T.J. Dhilip Kumar, Journal of Alloys and Compounds, 552 (2013) 457.
26. F. Buendía and M.R. Beltrán, Computational and Theoretical Chemistry, 1021 (2013) 183.
27. S. Zhao, X. Tian, J. Liu, Y. Ren and J. Wang, Computational and Theoretical Chemistry, 1055 (2015) 1.
28. R. Trivedi and D. Bandyopadhyay, International Journal of Hydrogen Energy, 40 (2015) 12727.
29. Y. Zhang and Z. Yang, Computational and Theoretical Chemistry, 1071 (2015) 39.
30. Y.-N. Li, Y.-B. Xie and C.-J. Liu, Catalysis Letters, 125 (2008) 130.
31. I.S. Bondarchuk and G.V. Mamontov, Kinetics and Catalysis, 56 (2015) 379.
32. Y. He, Y. Liu, P. Yang, Y. Du, J. Feng, X. Cao, J. Yang and D. Li, Journal of Catalysis, 330 (2015) 61.
33. C. Hu, X. Mu, J. Fan, H. Ma, X. Zhao, G. Chen, Z. Zhou and N. Zheng, ChemNanoMat, 2 (2016) 28.
34. F. Yao, X. Li, C. Wan, L. Xu, Y. An, M. Ye and Z. Lei, Applied Surface Science, 426 (2017) 605.
35. S.T. Nguyen, H.M. Law, H.T. Nguyen, N. Kristian, S. Wang, S.H. Chan and X. Wang, Applied Catalysis B: Environmental, 91 (2009) 507.

36. Y. Wang, Z.M. Sheng, H. Yang, S.P. Jiang and C.M. Li, International Journal of Hydrogen Energy, 35 (2010) 10087.
37. M.C. Oliveira, R. Rego, L.S. Fernandes and P.B. Tavares, Journal of Power Sources, 196 (2011) 6092.
38. S. Chen, B.D. Adams and A. Chen, Electrochimica Acta, 56 (2010) 61.
39. J. Okazaki, T. Ikeda, D.A.P. Tanaka, K. Sato, T.M. Suzuki and F. Mizukami, Journal of Membrane Science, 366 (2011) 212.
40. R. Song, Z. Zhang, C. Wang, H. Li and Z. Wang, Acta Metallurgica Sinica (English Letters), 26 (2013) 361.
41. J. Tang, S. Yamamoto, T. Koitaya, Y. Yoshikura, K. Mukai, S. Yoshimoto, I. Matsuda and J. Yoshinobu, Applied Surface Science, 463 (2019) 1161.
42. B. Sharma and J.-S. Kim, International Journal of Hydrogen Energy, 42 (2017) 25446.
43. S. Nigam and C. Majumder, Chemical Physics Letters, 537 (2012) 69.
44. A. Posada-Borbón and A. Posada-Amarillas, Chemical Physics Letters, 618 (2015) 66.
45. F. Al-Odail, J. Mazher and A.M. Abuelela, Computational and Theoretical Chemistry, 1125 (2018) 103.
46. M. Sandoval, P. Bechthold, V. Orazi, E.A. González, A. Juan and P.V. Jasen, Applied Surface Science, 435 (2018) 568.
47. Y. Zhao, M. Zhu and L. Kang, Journal of Molecular Graphics and Modelling, 83 (2018) 129.
48. R. Zhang, M. Xue, B. Wang and L. Ling, Applied Surface Science, 481 (2019) 421.
49. B. Han, L. Ling, R. Zhang, P. Liu, M. Fan and B. Wang, Molecular Catalysis, 484 (2020) 110731.
50. Y. Wang, B. Wang, L. Ling, R. Zhang and M. Fan, Chemical Engineering Science, 218 (2020) 115549.
51. M. Yang, B. Wang, M. Fan and R. Zhang, Chemical Engineering Science, 229 (2021) 116016.
52. S. Zhao, Y. Ren, Y. Ren, J. Wang and W. Yin, Journal of Molecular Structure: THEOCHEM, 955 (2010) 66.
53. S. Zhao, Y. Ren, Y. Ren, J. Wang and W. Yin, Computational and Theoretical Chemistry, 964 (2011) 298.
54. L.-D. Meng and G.-C. Wang, Phys. Chem. Chem. Phys., 16 (2014) 17541.
55. D. Liu, Applied Surface Science, 386 (2016) 125.
56. D. Palagin and J.P.K. Doye, Phys. Chem. Chem. Phys., 17 (2015) 28010.
57. Gaussian 09, Revision D.01, M. J. Frisch, G. W. Trucks, H. B. Schlegel, G. E. Scuseria, M. A. Robb, J. R. Cheeseman, G. Scalmani, V. Barone, B. Mennucci, G. A. Petersson, H. Nakatsuji, M. Caricato, X. Li, H. P. Hratchian, A. F. Izmaylov, J. Bloino, G. Zheng, J. L. Sonnenberg, M. Hada, M. Ehara, K. Toyota, R. Fukuda, J. Hasegawa, M. Ishida, T. Nakajima, Y. Honda, O. Kitao, H. Nakai, T. Vreven, J. A. Montgomery, Jr., J. E. Peralta, F. Ogliaro, M. Bearpark, J. J. Heyd, E. Brothers, K. N. Kudin, V. N. Staroverov, R. Kobayashi, J. Normand, K. Raghavachari, A. Rendell, J. C. Burant, S. S. Iyengar, J. Tomasi, M. Cossi, N. Rega, J. M. Millam, M. Klene, J. E. Knox, J. B. Cross, V. Bakken, C. Adamo, J. Jaramillo, R. Gomperts, R. E. Stratmann, O. Yazyev, A. J. Austin, R. Cammi, C. Pomelli, J. W. Ochterski, R. L. Martin, K. Morokuma, V. G. Zakrzewski, G. A. Voth, P. Salvador, J. J. Dannenberg, S. Dapprich, A. D. Daniels, Ö. Farkas, J. B. Foresman, J. V. Ortiz, J. Cioslowski, and D. J. Fox, *Gaussian 09* (Gaussian, Inc., Wallingford CT, 2009).
58. GaussView, Version 5, Roy Dennington, Todd A. Keith, and John M. Millam, Semichem Inc., Shawnee Mission, KS, 2009.
59. W. Bouderbala, A.-G. Boudjahem and A. Soltani, Molecular Physics, 112 (2014) 1789.
60. J.-Q. Wen, T. Xia, H. Zhou and J.-F. Wang, Journal of Physics and Chemistry of Solids, 75 (2014) 528.

61. D.A. Kilimis and D.G. Papageorgiou, The European Physical Journal D, 56 (2010) 189.
62. N. M. O'boyle, A. L. Tenderholt, and K. M Langner, *Journal of computational chemistry*, 29 (5) (2008) 839.

Tables

Table (1): The calculated bond length, r (Å), binding energy, E_b (eV) and vibrational frequency, ω (cm^{-1}) of Pd_2, Ag_2, Pd-Ag, Pd-H, Ag-H and H_2 dimers with other theoretical data and experimental values.

Dimer	Parameter	This Work			Theoretical *	Experimental
		B3LYP	B3P86	PW91PW91		
Pd-Pd	r	2.536	2.494	2.504	2.510 (B3PW91) [a] , 2.509 (BPW91) [b]	2.480 [a]
	E_b	0.318	0.477	0.746		0.366 [a] , 0.515 [a]
	ω	197.5	215.4	208.4	0.380 (B3PW91) [a] , 0.650 (BPW91) [b]	
					203.6 (B3PW91) [a] , 204.5 (B3LYP) [c]	210±10 [a] , 210.0 [c]
Ag-Ag	r	2.611	2.575	2.583	2.626 (BLYP) [d] , 2.598 (PBE) [d]	2.534 [d]
	E_b	0.776	0.812	0.891	0.825 (BLYP) [d] , 0.858 (PBE) [d]	0.825 [d]
	ω	177.2	190.0	186.8	172.1 (BLYP) [d] , 179.2 (PBE) [d]	192.4 [d]
Pd-Ag	r	2.612	2.581	2.584	2.598 (PBE0) [e] , 2.618 (B3LYP) [e] , 2.596 (BPW91) [e]	-
	E_b	0.577	0.594	0.768		-
	ω	177.8	186.6	185.8	0.553 (PBE0) [e] , 0.573 (B3LYP) [e] , 0.682 (BPW91) [e]	-
					178.6 (PBE0) [e] , 174.3 (B3LYP) [e] , 185.5 (BPW91) [e]	
Pd-H	r	1.537	1.525	1.529	1.548 (BH&H) [f] , 1.555 (RPBE) [g]	1.534 [f, g] , 1.529 [g]
	E_b	1.259	1.298	1.345	1.125 (RPBE) [g]	
	ω	2031.8	2092.2	2078.3	2011.6 (BH&H) [f]	1.195 ± 0.13 [g]
						2036 [f]
Ag-H	r	1.625	1.613	1.611	1.637 (BH&H) [f] , 1.631 (B3LYP) [h]	1.618 [f]
	E_b	1.139	1.192	1.173	1.249 (GGA-PW91) [l]	-
	ω	1706.7	1751.6	1738.3	1768.5 (BH&H) [f]	1759.7 [f] , 1717 [h]
H-H	r	0.744	0.745	0.750	0.749 (BH&H) [f] , 0.744 (B3LYP) [c]	0.741 [f] , 0.746 [c]
	E_b	2.382	2.422	2.271	2.340 (RPBE) [g]	
	ω	4418.1	4417.9	4331.5	4431.4 (BH&H) [f] , 4418.9 (B3LYP) [c]	2.240 [g]
						4401.2 [f]

*: The density functionals are shown between brackets.

a: [59]

b: [60]

c: [19]

d: [61]

e: [3]

f: [23]

g: [22]

h: [18]

I: [24]

Table 2: The spin multiplicity (M), the total energy difference (**ΔE**), adsorption energy (AE), shortest M-H bond length (R_{M-H}), H-H bond length (R_{H-H}), sum of NBO net charges of hydrogen atoms (q_{H2}) and HOMO-LUMO energy gap (E_{gap}) of the lowest energy structures of hydrogen adsorption and dissociation on single Pd and Ag atoms.

Cluster	M	ΔE (eV)	AE (eV)	R_{M-H} (Å)	R_{H-H} (Å)	q_{H2} (e)	E_{gap} (eV)
PdH_2_a	1	0	0.902	1.661	0.881	- 0.064	3.979 (2.618)
PdH_2_b	1	0.197	0.704	1.512	1.637	- 0.056	4.609
PdH_2_c	1	2.415	- 1.513	1.627	-	- 0.509	1.642
AgH_2_a	2	0	- 1.475	1.660	2.840	- 0.379	5.131 (4.817)
AgH_2_b	2	0.390	- 1.866	1.723	-	- 0.179	7.510

Table 3: The spin multiplicity (M), the total energy difference (ΔE_t), adsorption energy (AE), shortest M-M bond length (R_{M-M}), shortest M-H bond length (R_{M-H}), H-H bond length (R_{H-H}), sum of NBO net charges of hydrogen atoms (q_{H2}) and HOMO-LUMO energy gap (E_{gap}) of the lowest energy structures of hydrogen adsorption and dissociation on Pd_nAg_m dimers.

Cluster	M	ΔE_t (eV)	AE (eV)	R_{M-M} (Å)	R_{M-H} (Å)	R_{H-H} (Å)	q_{H2} (e)	E_{gap} (eV)
Pd_2H_2_a	1	0	1.974	2.699	1.661	1.939	- 0.281	3.834
Pd_2H_2_b	1	0.818	1.156	2.657	1.570	1.036	- 0.119	3.210
Pd_2H_2_c	1	1.501	0.473	2.738	1.681	0.870	- 0.053	1.596
$PdAgH_2$_a	2	0	0.505	2.653	1.708	0.849	0.001	3.332
$PdAgH_2$_b	2	0.117	0.387	2.664	1.770	0.825	- 0.027	4.111
$PdAgH_2$_c	2	0.467	0.038	2.567	2.426	0.753	0.016	3.405
$PdAgH_2$_d	2	0.389	0.116	2.602	1.609 (Pd) 1.873 (Ag)	-	- 0.589	2.128
$PdAgH_2$_e	2	0.398	0.107	2.723	1.578 (Pd) 1.752 (Ag)	-	- 0.505	3.121
$PdAgH_2$_f	2	0.609	- 0.105	2.687	1.585 (Pd) 1.627 (Ag)	-	- 0.524	4.226
Ag_2H_2_a	1	0	0.019	2.573	2.519	0.751	0.017	3.292
Ag_2H_2_b	1	1.425	- 1.406	2.528	1.976	-	- 1.087	2.648

Table 4: The spin multiplicity (M), the total energy difference (ΔE_t), adsorption energy (AE), average M-M bond lengths (R_{ABL}), shortest M-M bond length (R_{M-M}), shortest M-H bond length (R_{M-H}), H-H bond length (R_{H-H}), sum of NBO net charges of hydrogen atoms (q_{H2}) and HOMO-LUMO energy gap (E_{gap}) of the lowest energy structures of hydrogen adsorption and dissociation on Pd_nAg_m trimers.

Cluster	M	ΔE_t (eV)	AE (eV)	R_{ABL} (Å)	R_{Pd-Pd} (Å)	R_{Ag-Ag} (Å)	R_{Pd-Ag} (Å)	R_{M-H} (Å)	R_{H-H} (Å)	q_{H2} (e)	E_{gap} (eV)
Pd_3H_2_a	1	0	2.010	2.727	2.715	-	-	1.650	-	-0.266	2.871
Pd_3H_2_b	1	0.008	2.002	2.694	2.692	-	-	1.793	-	-0.255	3.274
Pd_3H_2_c	1	0.071	1.939	2.723	2.632	-	-	1.616	-	-0.233	2.765
Pd_3H_2_d	1	1.404	0.606	2.575	2.561	-	-	1.670	0.866	0.078	1.746
Pd_2AgH_2_a	2	0	0.641	2.765	2.675	-	2.807	1.678 (Pd) 2.212 (Ag)	-	-0.300	2.044
Pd_2AgH_2_b	2	0.140	0.502	2.710	2.756	-	2.655	1.599 (Pd) 1.966 (Ag)	-	-0.476	2.210
Pd_2AgH_2_c	2	0.163	0.478	2.630	2.550	-	2.628	1.732	0.836	0.043	3.398
Pd_2AgH_2_d	2	0.175	0.466	2.717	2.777	-	2.687	1.620 (Pd) 1.914 (Ag)	-	-0.607	2.445
Pd_2AgH_2_e	2	0.455	0.186	2.700	2.656	-	2.722	1.650	0.945	-0.059	2.566
$PdAg_2H_2$_a	1	0	0.619	2.682	-	2.666	2.668	1.730	0.840	0.009	3.066
$PdAg_2H_2$_b	1	0.025	0.594	2.683	-	2.667	2.670	1.727	0.837	0.003	2.937
$PdAg_2H_2$_c	1	0.418	0.201	2.789	-	3.161	2.603	1.687 (Pd) 1.937 (Ag)	-	-0.602	3.107
$PdAg_2H_2$_d	1	0.895	-0.276	2.727	-	2.789	2.640	1.560 (Pd) 1.635 (Ag)	-	-0.622	2.852
$PdAg_2H_2$_e	1	0.955	-0.337	2.740	-	2.603	2.772	1.645 (Pd) 1.828 (Ag)	-	-0.837	2.163
$PdAg_2H_2$_f	1	1.035	-0.416	2.702	-	2.604	2.751	1.544 (Pd) 1.912 (Ag)	-	-0.732	2.477
Ag_3H_2_a	2	0	0.095	2.759	-	2.656	-	2.218	0.761	0.031	1.651

Ag_3H_2_b	2	0.226	-0.131	2.773	-	2.732	-	1.786	-	-0.878	2.661	

Table 5: The spin multiplicity (M), the total energy difference (ΔE_t), adsorption energy (AE), average M-M bond lengths (R_{ABL}), shortest M-M bond length (R_{M-M}), shortest M-H bond length (R_{M-H}), H-H bond length (R_{H-H}), sum of NBO net charges of hydrogen atoms (q_{H2}) and HOMO-LUMO energy gap (E_{gap}) of the lowest energy structures of hydrogen adsorption and dissociation on Pd_nAg_m tetramers.

Cluster	M	ΔE_t (eV)	AE (eV)	R_{ABL} (Å)	R_{Pd-Pd} (Å)	R_{Ag-Ag} (Å)	R_{Pd-Ag} (Å)	R_{M-H} (Å)	R_{H-H} (Å)	q_{H2} (e)	E_{gap} (eV)
Pd_4H_2_a	1	0	1.285	2.771	2.701	-	-	1.691	-	-0.243	2.569
Pd_4H_2_b	1	0.035	1.250	2.752	2.701	-	-	1.631	-	-0.174	2.204
Pd_4H_2_c	3	0.820	0.465	2.637	2.558	-	-	1.764	0.823	0.054	3.444
Pd_3AgH_2_a	2	0	0.478	2.677	2.594	-	2.677	1.758	0.827	0.036	3.085
Pd_3AgH_2_b	2	0.056	0.422	2.744	2.748	-	2.708	1.648	-	-0.357	1.872
Pd_3AgH_2_c	2	0.090	0.387	2.743	2.740	-	2.706	1.594	-	-0.408	2.242
Pd_3AgH_2_d	2	0.403	0.075	2.662	2.603	-	2.721	2.237	0.758	0.032	3.407
Pd_3AgH_2_e	2	0.739	-0.261	2.726	2.626	-	2.824	1.632	-	-0.601	3.240
$Pd_2Ag_2H_2$_a	1	0	0.620	2.723	2.744	2.785	2.663	1.721	0.841	0.010	2.476
$Pd_2Ag_2H_2$_b	1	0.472	0.147	2.771	2.746	2.679	2.739	1.561	1.821	-0.178	2.206
$Pd_2Ag_2H_2$_c	1	0.548	0.072	2.710	2.711	2.822	2.680	2.248	0.758	0.029	2.393
$Pd_2Ag_2H_2$_d	1	0.583	0.037	2.764	2.756	2.852	2.691	1.637	-	-0.515	2.710
$Pd_2Ag_2H_2$_e	1	0.745	-0.125	2.762	2.736	2.647	2.797	1.653	-	-0.661	2.559
$PdAg_3H_2$_a	2	0	0.565	2.725	-	2.695	2.716	1.738	0.835	0.046	2.643
$PdAg_3H_2$_b	2	0.200	0.365	2.750	-	2.781	2.691	1.681	-	-0.530	2.159
$PdAg_3H_2$_c	2	0.490	0.075	2.705	-	2.742	2.666	2.254	0.759	0.036	2.579
$PdAg_3H_2$_d	2	0.540	0.025	2.749	-	2.683	2.760	1.651	-	-0.688	3.652
$PdAg_3H_2$_e	4	2.876	-2.310	2.794	-	2.754	2.764	1.641	-	-0.371	2.708
Ag_4H_2_a	1	0	0.452	2.760	-	2.722	-	1.816	-	-0.897	3.720
Ag_4H_2_b	1	0.291	0.162	2.740	-	2.631	-	2.101	0.769	0.047	2.303
Ag_4H_2_c	3	1.626	-1.174	2.865	-	2.745	-	1.754	-	-0.851	1.898

Figures

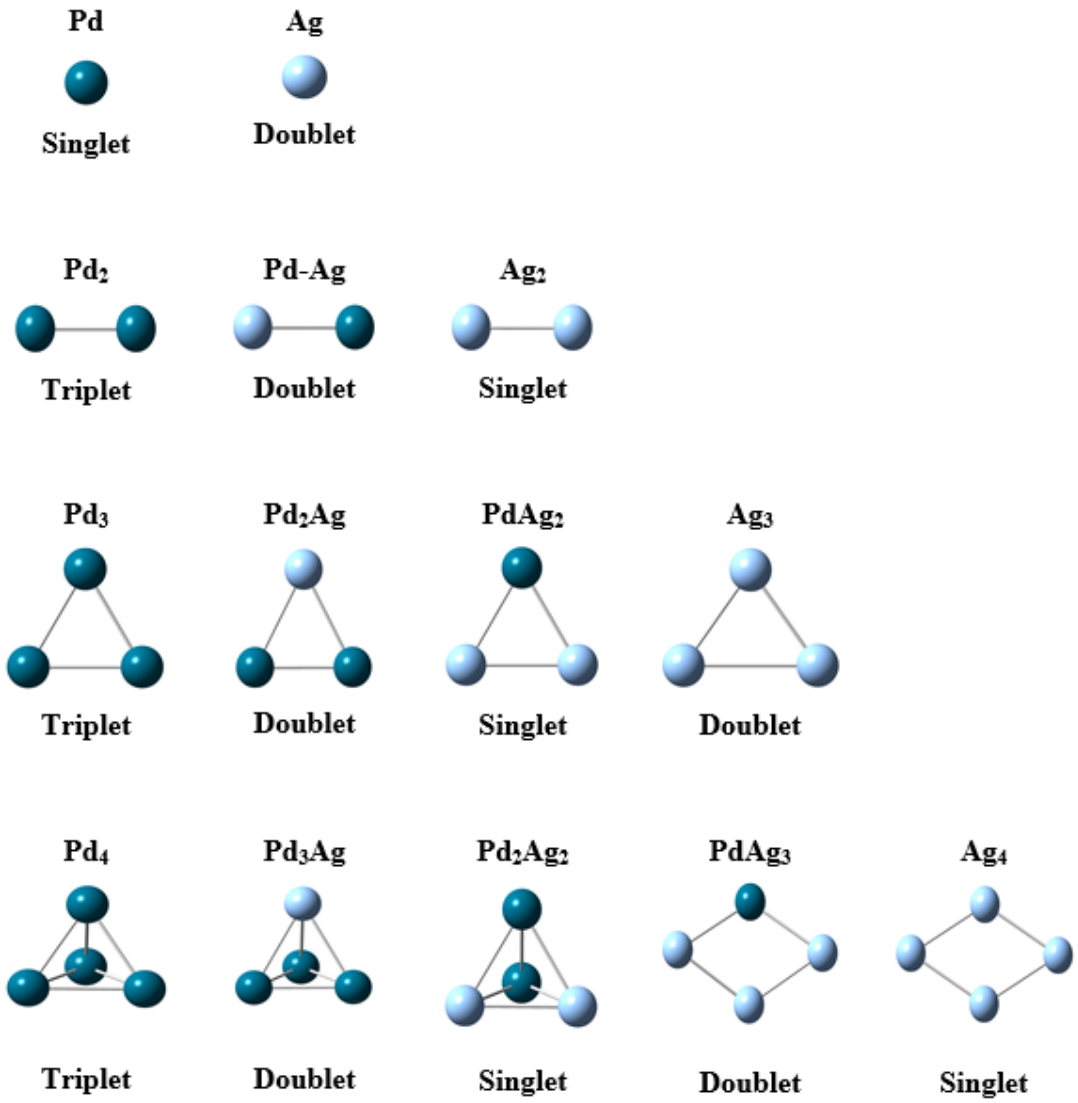

Figure 1

The lowest energy structures of small Pd, Ag and Pd_nAg_m clusters. The spin multiplicity is shown for each structure. Blue balls correspond to Pd atoms, while light blue balls correspond to Ag atoms.

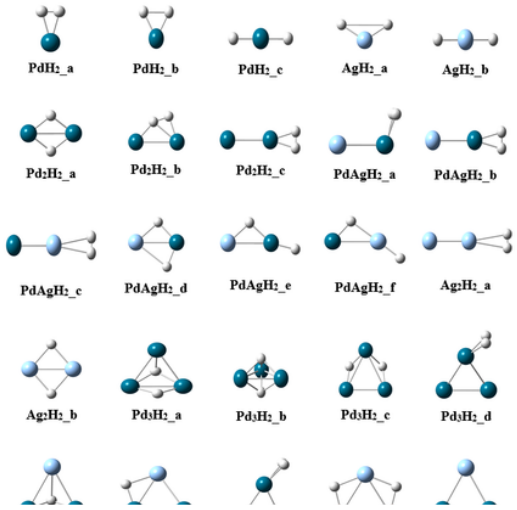

Figure 2

The lowest energy structures (a) and other low-lying isomers (b-f) of hydrogen adsorption and dissociation on Pd_nAg_m clusters arranged from the highest to lowest Pd content in the cluster and lowest to highest energy structures.

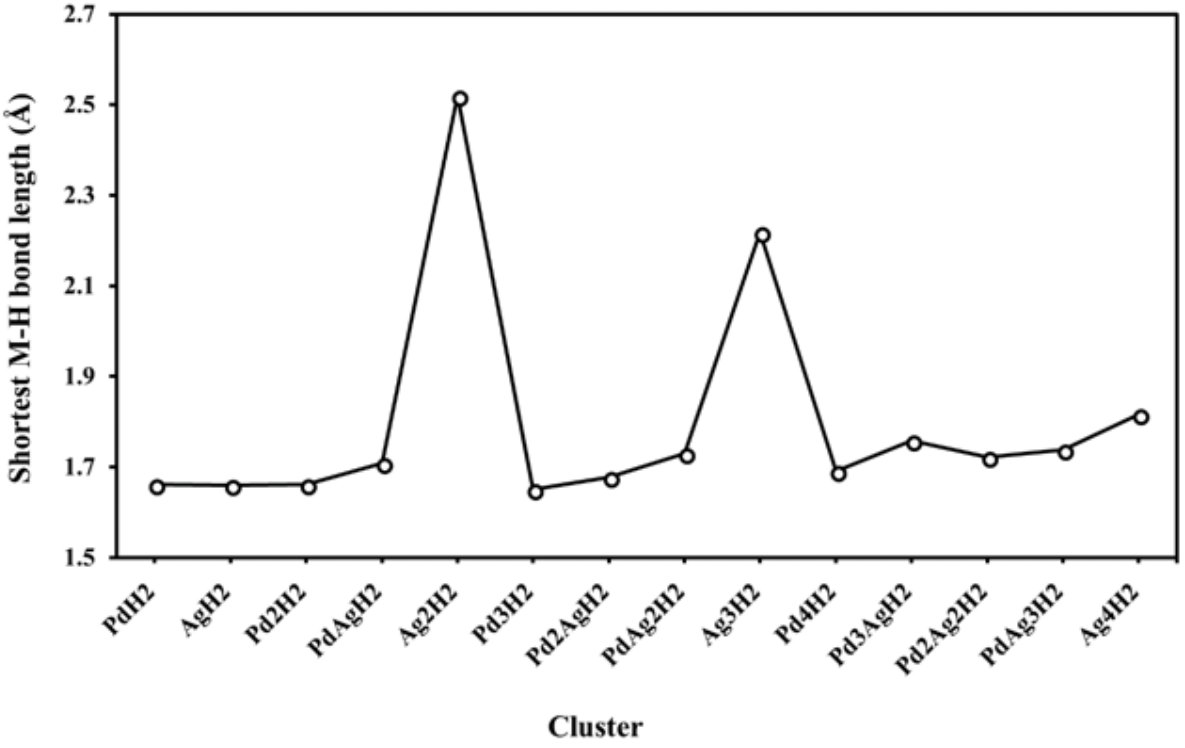

Figure 3

The shortest M-H bond length of the most stable structures of Pd_nAg_m-H_2 clusters

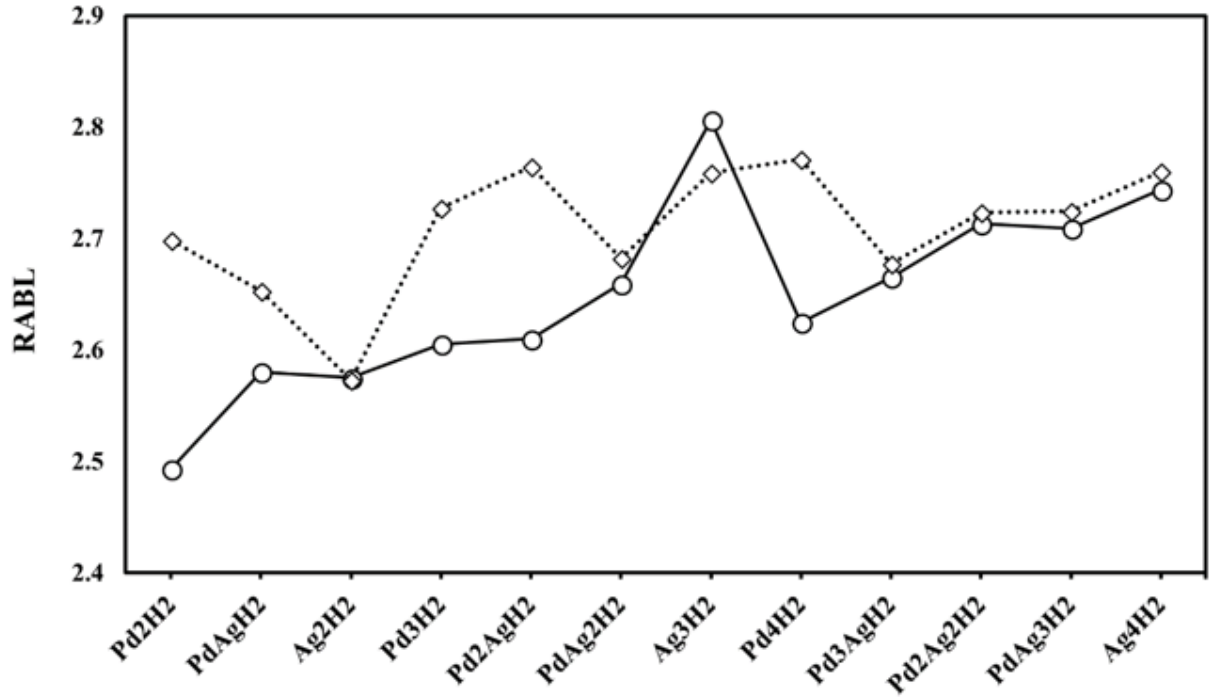

Figure 4

The average M-M bond lengths (R_{ABL}) of the lowest energy structures of Pd_nAg_m clusters before (solid line) and after the interaction with H_2 (dotted line).

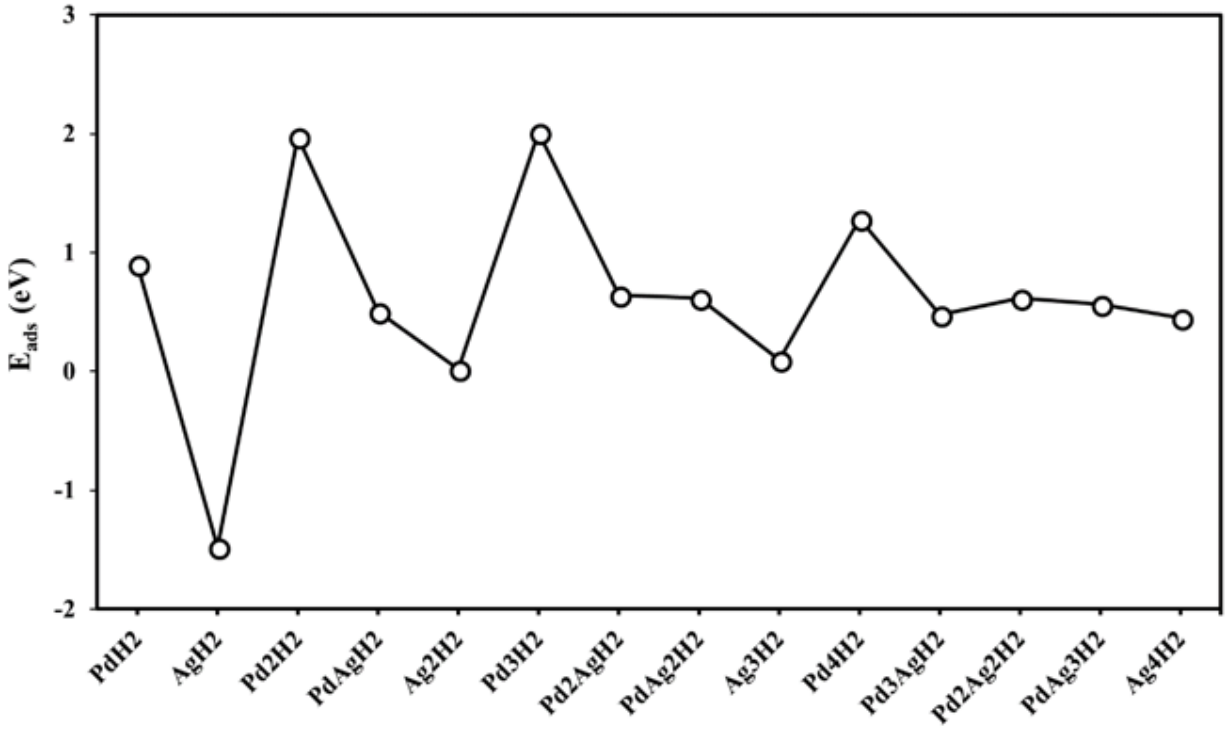

Figure 5

The adsorption energies (E_{ads}) for the ground state geometries of Pd_nAg_m-H_2 clusters.

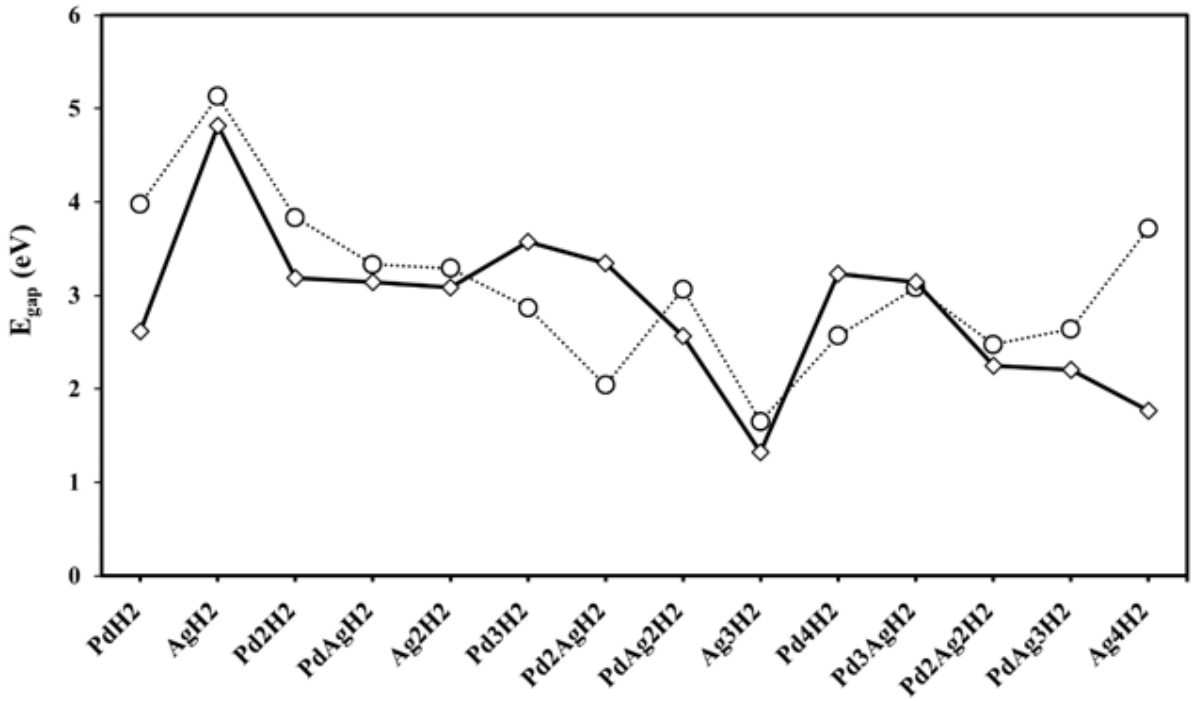

Figure 6

The HOMO-LUMO energy gap (E_{gap}) of the ground state structures of Pd_nAg_m (solid line) and Pd_nAg_m-H_2 (dotted line) clusters.

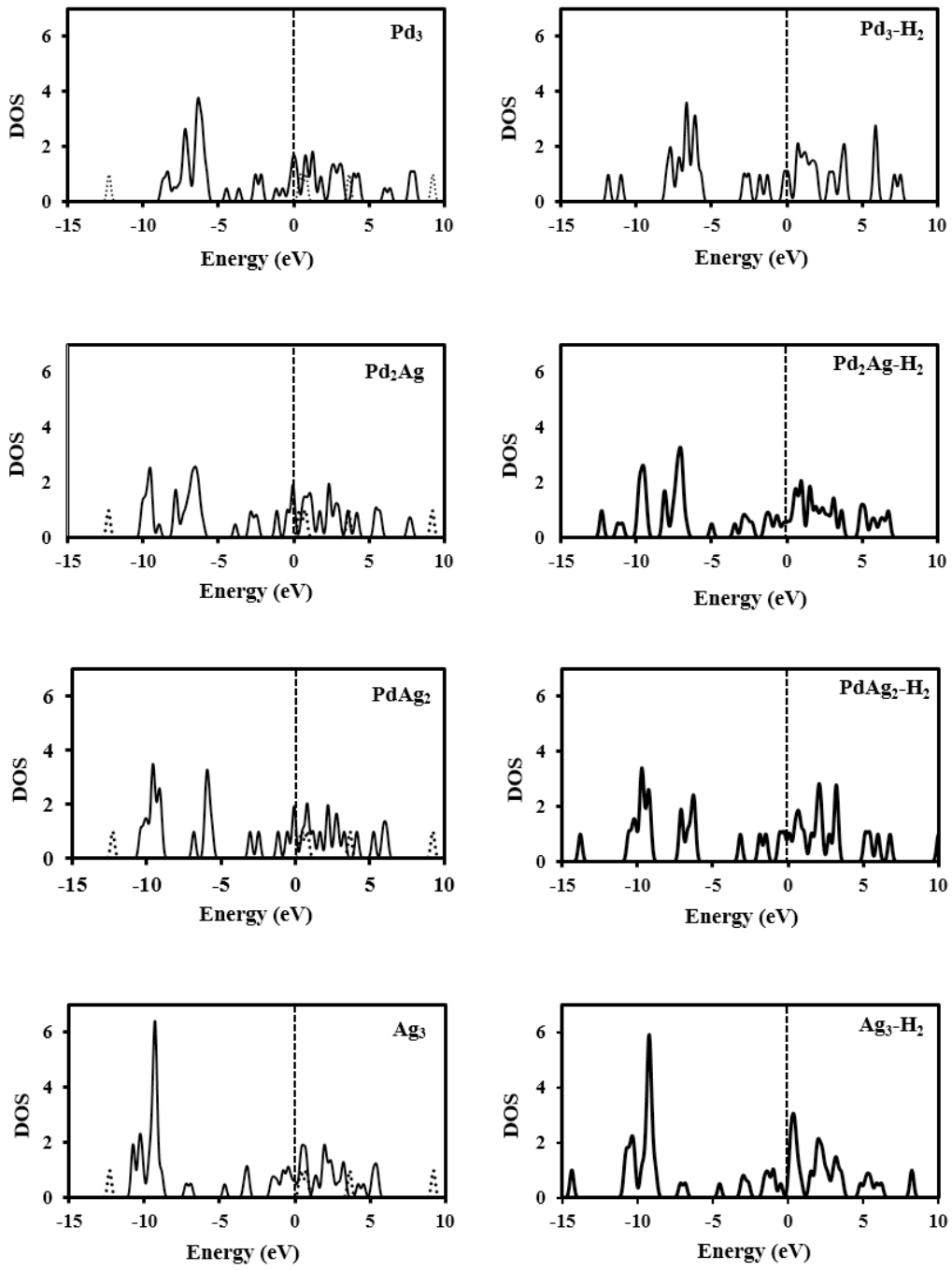

Figure 7

The electronic density of state (DOS) of the Pd_nAg_m and Pd_nAg_m-H_2 trimers (solid lines) and hydrogen molecule in the gas phase (dotted lines). The dashed line refers to the Fermi level.